

Stable vortex structures in colliding self-gravitating Bose-Einstein condensates

Y. O. Nikolaieva^{1,2,3}, Y. M. Bidasyuk², K. Korshynska^{1,2}, E. V. Gorbar^{1,4}, Junji Jia⁵, and A. I. Yakimenko^{1,6,7}

¹*Department of Physics, Taras Shevchenko National University of Kyiv, 64/13, Volodymyrska Street, Kyiv 01601, Ukraine*

²*Physikalisch-Technische Bundesanstalt (PTB), Bundesallee 100, D-38116 Braunschweig, Germany*

³*Vienna Center for Quantum Science and Technology, Atominstitut, TU Wien, Stadionallee 2, 1020 Vienna, Austria*

⁴*Bogolyubov Institute for Theoretical Physics, 14-b Metrolohichna Street, Kyiv 03143, Ukraine*

⁵*School of Physics and Technology, Wuhan University, 299 Bayi Road, Wuhan, Hubei Province, 430072, China*

⁶*Dipartimento di Fisica e Astronomia 'Galileo Galilei', Università di Padova, via Marzolo 8, 35131 Padova, Italy*

⁷*Istituto Nazionale di Fisica Nucleare, Sezione di Padova, via Marzolo 8, 35131 Padova, Italy*



(Received 5 January 2023; accepted 12 June 2023; published 5 July 2023)

A key feature of ultralight dark matter composed by bosons is the formation of superfluid Bose-Einstein condensate (BEC) structures on galactic scales. We study collisions of BEC solitonic and vortex structures in the framework of the Gross-Pitaevskii-Poisson model. It is found that the superfluid nature of bosonic dark matter leads to the formation of quantized vortex lines and vortex rings in interference patterns formed during collisions. Calculating the gravitational wave luminosity, we demonstrate that quantum interference patterns affect notably gravitational wave radiation. We reveal that superfluid self-gravitating BECs can form stable localized vortex structures which remain robust even after a head-on collision.

DOI: [10.1103/PhysRevD.108.023503](https://doi.org/10.1103/PhysRevD.108.023503)

I. INTRODUCTION

The nature, composition, and physical properties of dark matter (DM) are key puzzles of modern physics, astrophysics, and cosmology. DM composed by ultralight bosons in the state of Bose-Einstein condensate (BEC) presents an appealing possibility because it naturally resolves some problems of the standard Λ CDM model on the galactic scale while maintaining the success of the latter on larger scales (for a review, see [1]). These conclusions are well-supported by cosmological simulations [2]. The large-scale structure of the ultralight DM simulations is indistinguishable from CDM, being consistent with astrophysical observations. In cosmological studies, it was found that the boson mass has to be ultralight to reproduce the observed distribution of matter at large scales [3,4]. For such extremely small mass, namely, of the order of $m \sim 10^{-22}$ eV [2], quantum mechanical phenomena manifest themselves on galactic scales. The viability of the fuzzy DM model, a kind of ultralight DM without self-interaction, was studied with the stellar kinematics measurements in dwarf galaxies [5].

The evolution of a self-gravitating galactic BEC is governed by the system of the Gross-Pitaevskii-Poisson (GPP) equations. These equations appear in different areas of physics and describe such seemingly distinct physical

processes as the nonlinear propagation of optical beams in nonlocal media, atomic BECs, and the evolution of cold DM galactic halos [6–9]. The theoretical proposal on how the interatomic interaction potential can be engineered to mimic gravitational interaction was first introduced in Ref. [10] and further developed in Refs. [11–13]. The central idea of these proposals is based on a dipole-dipole interaction between atoms modified by high-intensity off-resonant laser beams. This opens an intriguing possibility of modeling cosmological structures via their laboratory analogs, where the results obtained in one area can be applied in the others.

BEC structures could play an important role in astrophysics and cosmology. They have been predicted to form the central cores of ultralight axion DM halos. Similar proposals to describe DM structures as BEC were suggested in many studies [14–18].

A well-established fact is that compact spherical astrophysical objects that may be formed due to the Bose-Einstein condensation of DM are stable, as was found numerically [19,20]. Since BEC is a superfluid, it could form vortices with quantized angular momentum [21,22]. Rotation in BEC halos would affect their structure and thus could lead to observable consequences [18,23–25].

Stationary vortex states of a spinning DM cloud with different winding numbers and typical galactic halo mass

and radius were recently studied in [26]. It was found that while all multicharged vortex states are unstable, a single-charged vortex state is very robust, even being strongly perturbed, and survives during the lifetime of the Universe. An analysis of the stability of solutions with different winding numbers and interaction constant values, e.g., bosonic stars, was performed in [27] where it was found that only states with winding number $s = 0$ and $s = 1$ could be stable. Furthermore, fundamental solitons form an interference pattern during a head-on collision, but survive and revive their shapes after collision [13,28–31]. This raises a more sophisticated question of whether the vortex solitons also remain stable after a head-on collision. To the best of our knowledge, stability of colliding vortex solitons in self-gravitating BEC has never been investigated.

An important clue to revealing DM nature is the first indication of DM nongravitational self-interaction, which has been recently reported for clusters collisions [32,33]. These observations could be explained by the ultralight DM model with collisional dynamics of stable solitary solutions of the Schrödinger-Poisson equation [34]. The nature of BEC severely affects the collisional dynamics of DM clumps and could explain the recent puzzling observations, presented in [32,33].

Binary solitonic collisions were studied both analytically and numerically [28]. These collisions are characterized by the relative amounts of the kinetic, self-interaction, and gravitational binding energies. Systems with “negative” energy (when the kinetic and self-interaction energies are smaller than the gravitational binding energy) will combine and merge, whereas systems with “positive” energy will behave as solitons and pass right through each other. The 3D cosmological simulations with merging multiple solitons to create individual virialized objects were conducted [33,35–37]. During the merger of two-state configurations, the total density approaches a stationary state. The obtained averaged profile has a core plus tail structure that could serve to explain the results in simulations of DM structure formation [33,36]. Similar numerical solutions were obtained in the case of collision of two spherical BEC cores, with [38] and without [36,39] the nonlinear self-interaction term in the GPP equations. In collisions of solitonic cores with opposite phases, a destructive interference occurs, which gives rise to a short-range repulsive force between the cores [34]. As the authors of [32] pointed out in the context of galaxy cluster observations with indications of an offset between dark and stellar matter [32,40], this effect can provide an alternative explanation to self-interacting DM.

The relaxation process during BEC structures collision suggests a rich phenomenology [41]. Mergers of two solitons undergo relaxation in the form of gravitational cooling [36]. The gravitational cooling process for initially quite arbitrary density profiles leads to relaxation

and virialization through the emission of bosonic particles [42]. In addition, density oscillations take place and the period of these oscillations could range from a fraction of 1 gigayear up to many gigayears [36].

Alternative treatment of the soliton-soliton collision and orbiting binary boson stars is discussed in [43–45], where instead of the standard nonrelativistic GPP system of equations, the Einstein-Klein-Gordon system of equations is solved. The first studies of head-on collisions of mini bosonic stars were performed in [46] by using 3D code. Ultrarelativistic collisions were considered in [47], and head-on and orbital mergers of nonidentical boson stars in [43,44].

Obviously, since only the luminous matter is directly observable, collisions of galaxies composed of dark and luminous matter could provide very important information about DM [42]. Studies in this direction [42] show that luminous matter cannot follow these extreme dynamics and is expelled from the gravitational potential. The bullet cluster gives the famous example [48], in which the visible matter and DM are spatially separated after the collision. Therefore, it is interesting to determine the characteristics of collisions of self-gravitating BECs in states with nonzero angular momentum too. This provides the motivation for the study in this paper.

One of the potentially observable characteristics of the collision process is the emission of gravitational waves (GW). It is worth mentioning that GWs can allow us to find unexpected astrophysical compact objects with low brightness, known generically as exotic compact objects (ECOs). Among the most plausible ECO candidates are the bosonic stars, self-gravitating objects made of a complex scalar field [49,50]. Boson stars provide a simple and useful model to study compact bodies in different scenarios, such as DM candidates and black hole mimickers.

In this paper, we consider collisions of DM structures in the BEC state for different orientations of the angular momentum. We found that the BEC clouds after the formation of the interference pattern during the collision restore their topological structure even for an arbitrary impact parameter and the initial orientation of their vortex cores.

The paper is organized as follows. The model is described in Sec. II. Stationary fundamental soliton and single-charged vortex states are considered in Sec. III. Binary collisions are studied in Sec. IV. The emission of GWs produced by colliding superfluid DM structures is investigated in Sec. V. Conclusions are drawn in Sec. VI.

II. MODEL

At zero temperature, the dynamics of self-gravitating BEC of weakly interacting bosons in the mean-field approximation is described by the system of the GPP

equations for the BEC and gravitational potential, which in the dimensionless units takes the following form:

$$i \frac{\partial \Psi}{\partial t} = \left(-\frac{1}{2} \nabla^2 + \Phi + \nu |\Psi|^2 \right) \Psi, \quad (1)$$

$$\nabla^2 \Phi = |\Psi|^2, \quad (2)$$

where $\Psi(\mathbf{r}, t)$ is a complex wave function of the condensate, $\mathbf{r} = (x, y, z)$ is the vector of spatial coordinates, and t is time. The Gross-Pitaevskii equation (1) governing Ψ is a nonlinear Schrödinger equation with nonlinearity sourced by gravitational potential $\Phi(\mathbf{r}, t)$ and nonlocal interparticle interaction. Coefficient ν takes the value $+1$ for repulsive interparticle interaction, -1 for attractive interparticle interaction, and 0 if particles do not interact. In this work, we consider the case of repulsive interparticle interaction $\nu = 1$. The total energy associated with the GPP system of equations can be written as

$$E = \Theta + U + W, \quad (3)$$

where, in the dimensionless units, the kinetic energy is

$$\Theta = \frac{1}{2} \int |\nabla \Psi|^2 d\mathbf{r}, \quad (4)$$

the internal energy

$$U = \frac{1}{2} \int |\Psi|^4 d\mathbf{r}, \quad (5)$$

and the gravitational potential energy of interaction is given by

$$W = \frac{1}{2} \int |\Psi|^2 \Phi d\mathbf{r}. \quad (6)$$

To obtain dimensional quantities, one can use the following relations $\mathbf{r}_{\text{ph}} = \mathbf{r} L_*$, $t_{\text{ph}} = t / \Omega_*$, $\Phi_{\text{ph}} = \Phi \phi_*$, $\Psi_{\text{ph}} = \Psi \psi_*$, $E_{\text{ph}} = E \epsilon_*$, where $L_* = \lambda_C (m_{\text{pl}} / m) \sqrt{\lambda / 8\pi}$, $\Omega_* = c \lambda_C / L_*^2$, $\phi_* = (c \lambda_C / L_*)^2$, $\psi_* = mc^2 / ((\lambda / 8\pi) \times (m_{\text{pl}} / m)^2 \sqrt{4\pi G M \hbar})$, $\epsilon_* = \hbar^2 (8\pi / \lambda)^{3/2} / (4\pi m_{\text{pl}} \lambda_C^2)$, $m_{\text{pl}} = \sqrt{\hbar c / G}$ is the Planck mass, $\lambda / 8\pi = a_s / \lambda_C$ is the self-interaction constant with a_s being the s -wave scattering length, m is a particle mass, $\lambda_C = \hbar / mc$ is the Compton wavelength of bosons and M is the total BEC cloud mass.

The normalization constant N_s in dimensionless units is as follows:

$$\int |\Psi|^2 d\mathbf{r} = \frac{1}{\psi_*^2 L_*^3} = 4\pi \frac{M}{m_{\text{pl}}} \sqrt{\frac{\lambda}{8\pi}} = N_s. \quad (7)$$

Further, we fix $N_s = 100$, unless otherwise noted.

Before proceeding to the study of BEC DM structures collision, let us consider the properties of stationary self-gravitating BEC solitons.

III. STATIONARY STATES

As a result of the balance between gravitational attraction, quantum pressure, and repulsive bosonic interparticle interaction, the system of equations (1) and (2) allows the existence of stationary solutions with the wave function

$$\Psi(\mathbf{r}, t) = \psi(\mathbf{r}) e^{-i\mu t}, \quad (8)$$

where μ is the chemical potential and $\psi(\mathbf{r})$ is the spatial profile of the wave function. We seek for $\psi(\mathbf{r})$ in the form

$$\psi(r_{\perp}, \theta, z) = \chi(r_{\perp}, z) e^{is\theta},$$

where $r_{\perp} = \sqrt{x^2 + y^2}$, and the integer number s is the winding number.

In [26], we have analytically and numerically analyzed the stationary states with different winding numbers and investigated their stability. It has been found that the self-gravitating BEC states with $s = 0$ (the fundamental soliton) and $s = 1$ (the vortex soliton) can be stable even under strong perturbations, which is also in good agreement with the results obtained in [27]. For this work, we have developed an efficient numerical scheme for solving the system of equations (1), (2) in three spatial dimensions. Stationary states were numerically obtained by evolving the system (1), (2) in imaginary time with a normalization constraint. We therefore can use the same numerical methods for stationary states and for the dynamics of the system. The Gross-Pitaevskii equation is solved using the standard pseudo-spectral ‘‘split-step’’ method [51]. For the Poisson equation, we adapt the well-known geometric multigrid method. While the Poisson equation does not explicitly depend on time, the values of gravitational potential at every time step are obtained using a single multigrid V-cycle with 19-point Jacobi smoother [52–54], and using the result from a previous time step as an initial condition for the next one. Additionally, in order to keep the computational domain reasonably small, a careful consideration of boundary conditions for the Poisson equation is extremely important. We set the values of the potential Φ at the boundaries using a combination of monopole and quadrupole potentials

$$\Phi = -\frac{N_s}{4\pi r} - \frac{1}{8\pi r^5} \sum_{ij} I_{ij} x_i x_j,$$

where the quadrupole moment I_{ij}

$$I_{ij} = \int |\Psi|^2 \left(x_i x_j - \frac{1}{3} \delta_{ij} \mathbf{r}^2 \right) d\mathbf{r} \quad (9)$$

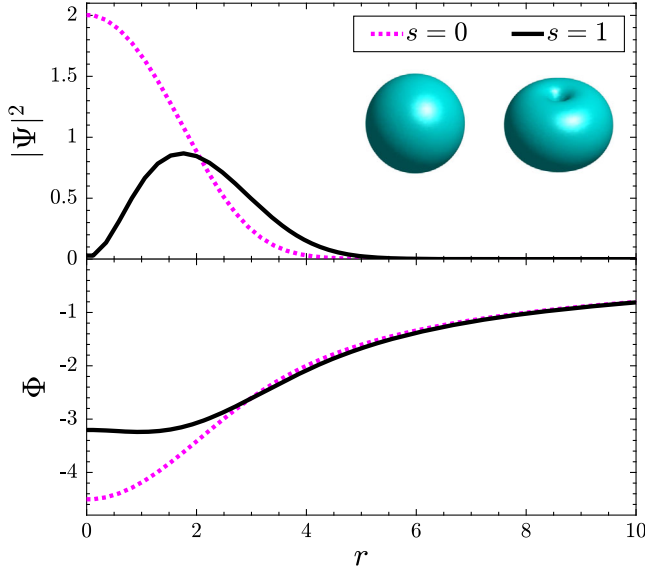


FIG. 1. Radial distribution of the stationary density distribution and gravitational potential in $z = 0$ plane for the BEC states $s = 0$ and $s = 1$ with normalization constant $N_s = 100$. The inset represents the corresponding 3D isosurfaces of condensate density.

is calculated from the current mass distribution and updated at every time step accordingly.

Figure 1 shows the density distribution $|\Psi|^2$ and the corresponding gravitational potential Φ for solutions with $s = 0$ and $s = 1$. As can be seen from the isosurfaces, the ground state solution is spherically symmetric, while the vortex has an axial symmetry. The peak density of the $s = 0$ state is higher than in the case of the vortex soliton, whose density is more spread and decreases to zero at the origin. The gravitational potential at this point has the global minimum in the case $s = 0$ and a local maximum in the case $s = 1$.

The parameters which characterize the system size can be defined as

$$R_0^2 = \frac{1}{N_s} \int r^2 |\Psi|^2 d\mathbf{r} \quad (10)$$

for the $s = 0$ state, where $r = \sqrt{x^2 + y^2 + z^2}$, and

$$R_1^2 = \frac{1}{N_s} \int r_{\perp}^2 |\Psi|^2 d\mathbf{r}, \quad (11)$$

$$Z_1^2 = \frac{1}{N_s} \int z^2 |\Psi|^2 d\mathbf{r} \quad (12)$$

for the $s = 1$ state. Figure 2 represents the total energy defined by Eq. (3), the chemical potential, determined by Eq. (8), and the system size characteristics given by Eqs. (10)–(12) as functions of normalization constant N_s . As one can see, the energy and chemical potential of the

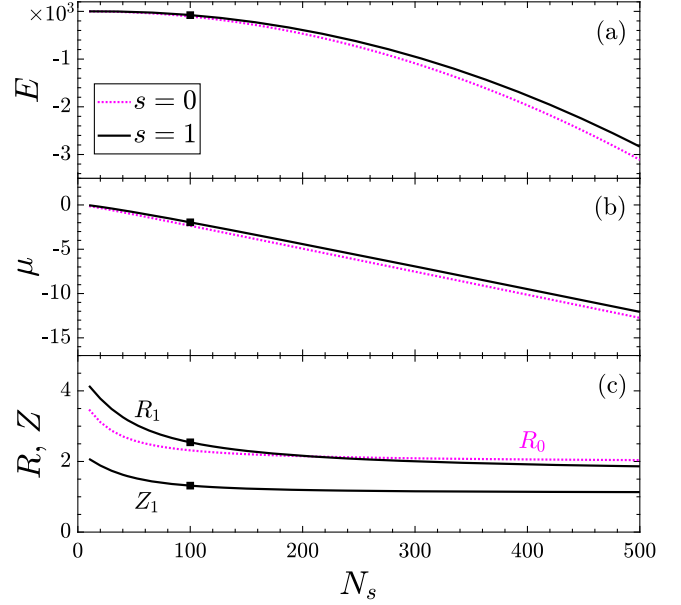


FIG. 2. (a) Total energy E , (b) chemical potential μ , (c) effective radius R , and height Z as functions of the normalization constant N_s for stationary states with winding numbers $s = 0$ and $s = 1$. Black dots show the corresponding values at $N_s = 100$.

vortex state are bigger due to additional rotational energy. The size of both systems decreases with the mass and approaches a constant value. Due to the vortex core structure, the mean width of the vortex state is approximately two times bigger than its height. The black dots mark the value corresponding to the normalization constant $N_s = 100$.

As it has been mentioned above, the two considered self-gravitating BEC states with $s = 0$ and $s = 1$ are quite robust, which makes it interesting to study their collision.

IV. BINARY COLLISIONS

Here, we consider the scattering of the solitons discussed in the previous section. Initially, we place two BEC clouds of the same mass at some distance from each other so that their wave functions do not overlap. We set the initial velocities along the z -axis by multiplying the wave functions by the appropriate exponents $\Psi = \Psi_1 \cdot e^{-ivz} + \Psi_2 \cdot e^{ivz}$. For sufficiently small initial velocities, condensate structures can merge and form a single blob. In all further cases, we consider initial dimensionless velocity $v = 1.5$ (in units of $L_* \Omega_*$) large enough to produce quasielastic collisions.

Let us first investigate the collision of two fundamental solitons ($s = 0$). During the merging, there appear such structures as vortex rings, which can be seen in Fig. 3. The cyan structures show the surfaces of the constant density value. The blue and black dots mark the centers of the vortex cores and represent oppositely rotating vortex rings. As can be seen, when approaching, pairs of oppositely

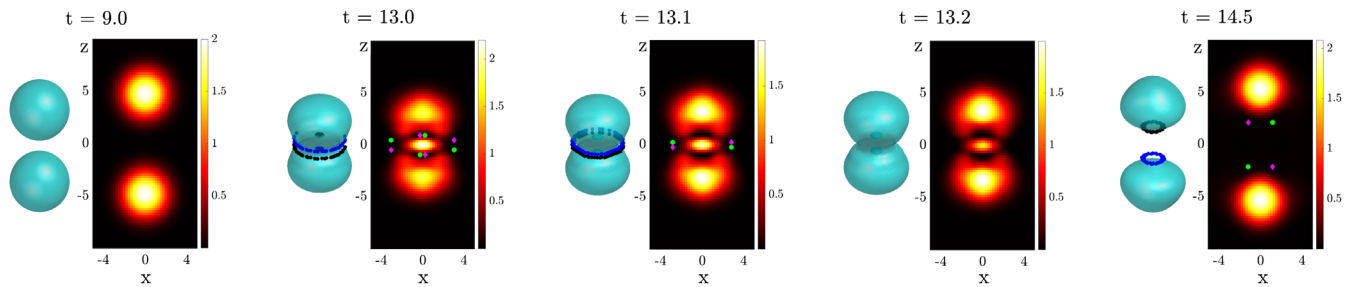


FIG. 3. A sequence of the density isosurfaces representing the dynamics of $s = 0$ solitons collision with the formation of oppositely rotating vortex rings (colored in blue and black). Snapshots show the density distribution in the plane ($y = 0$). Green dots represent the location of vortex cores, and magenta diamonds correspond to antivortex core location.

rotating vortex rings (marked in blue and black on the isosurfaces) are formed. Further, the inner rings shrink to a point and disappear. The outer pair of rings annihilates as they approach. The rings are again visible when the solitons move away.

Now let us consider collisions of single-charged vortex solitons ($s = 1$). The patterns appearing during the dynamics depend on the orientation of the vortices' angular momenta. Figure 4 shows the simulation of the collision dynamics of the vortices with angular momenta parallel to the collision axis. The upper row represents the case of the co-rotating superflows ($s_1 = 1, s_2 = 1$), while the lower row corresponds to the counter-rotating superflows ($s_1 = 1, s_2 = -1$). Blue and black dots indicate the location of the vortices' cores and their orientation. During merging, solitons interfere but pass through each other and revive their forms. As one can see in the case of oppositely oriented angular momenta, there appears a perpendicular vortex core (marked by magenta dots) similar to the well-known Josephson vortex (see e.g., [55])

which is responsible for the continuity of the wave function phase.

Further, we investigate another limiting case of the vortex cores' orientation during the scattering: perpendicular to the axis of collision. Figure 5 shows a collision of the corotational ($s_1 = 1, s_2 = 1$) and counter-rotational superflows ($s_1 = 1, s_2 = -1$), with angular momentum directed along the y -axis. In this configuration, an additional vortex appears in the case of corotational superflows collision. One can also see the complicated dynamics with vortex lines' recombination into the vortex rings. And as in the previous case, vortices recover their structure after the merging.

In all previous cases of the symmetric superflows orientation, solitons have not been destroyed despite the density redistribution during the collision. Therefore, it is interesting to investigate the interaction of vortices with arbitrarily directed angular momenta. It turns out that vortices revive after merging, even in the general case of the arbitrary orientation and nonzero impact parameter (the upper row in Fig. 6). We have also considered the collision

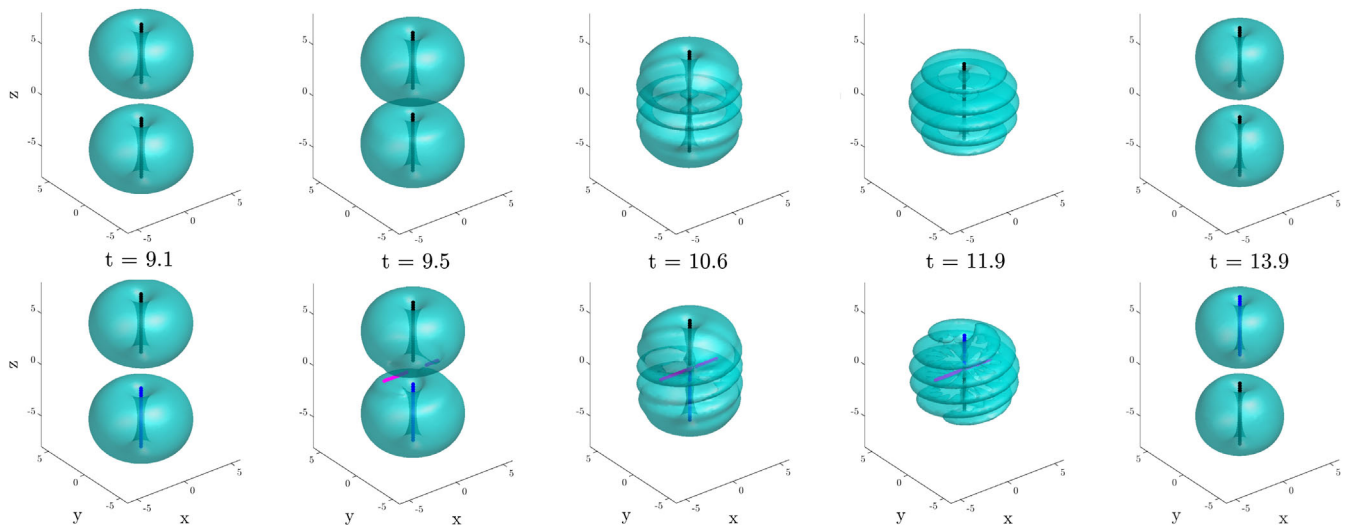


FIG. 4. Snapshots of head-on collision of BEC vortex states propagating along the vortex line direction. Shown are the condensate density isosurfaces for colliding vortex structures with the co-rotating (upper row) and counter-rotating (lower row) superflows. The dots represent the vortex cores' location, and their colors correspond to the direction of the superflow rotation.

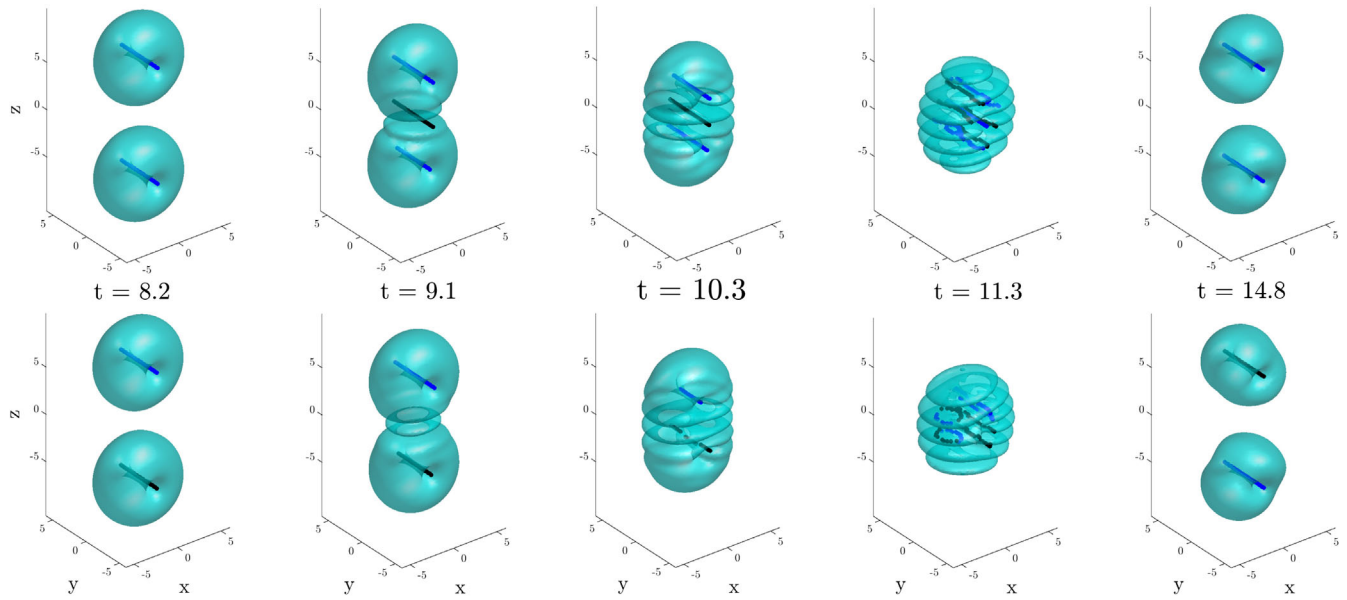


FIG. 5. The same as in Fig. 4 but with the angular momentum perpendicular to the collision axis. The upper row shows the colliding of corotating superflows, and the lower row represents the case of counter-rotating superflows.

of a vortex ($s_1 = 1$) and a fundamental soliton ($s_2 = 0$), which is shown on the lower row in Fig. 6. As in all previous cases, the solitons pass through each other without being destroyed. In these cases, we do not show the vortex cores, as the dynamic of collisions is complicated and governed by initial conditions.

Figure 7 shows the comparison between the merging dynamics of fundamental solitons (magenta line) and vortices moving along the direction of the vortex line (black

line). The upper panel represents the relative kinetic energy Θ/N , (where $N = 2N_s$ the total normalization constant of the system), which is higher in the case of vortex collision due to the nonzero angular momentum. Note that the final value of the kinetic energy is lower than the initial one, which illustrates that collision is not completely elastic. The lower panel shows the peak density of the system as a function of time. As can be seen, in the case of merging $s = 1$ vortex solitons, its variation is bigger.

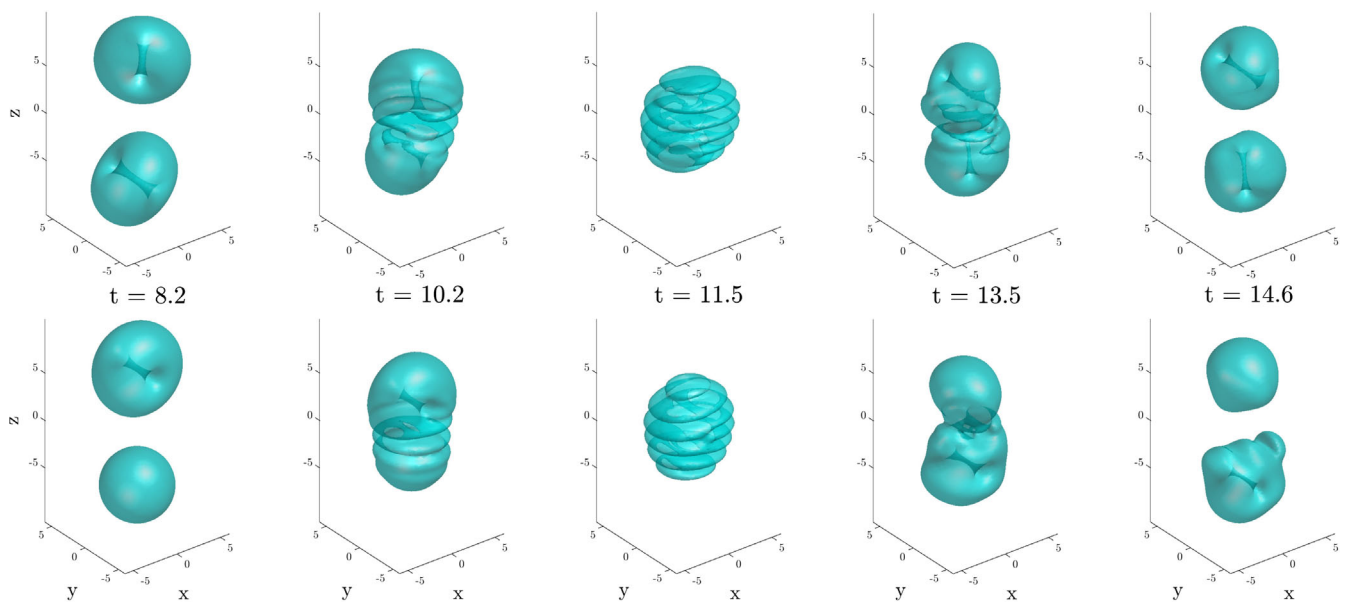


FIG. 6. The upper row demonstrates snapshots of the collision of two vortex states with arbitrary oriented angular momentum and nonzero impact parameter. The lower row shows the collision of the fundamental soliton and the vortex, with angular momentum perpendicular to the direction of movement.

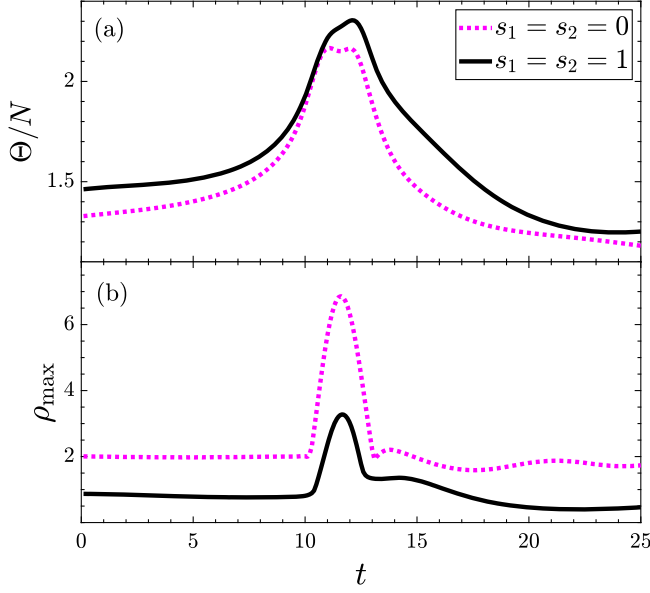


FIG. 7. (a) Kinetic energy per particle, (b) peak density value during the collision of two DM clouds. The magenta line represents the case of colliding solitons with winding numbers $s_1 = s_2 = 0$, while the black line corresponds to $s_1 = s_2 = 1$ vortices propagating along the direction of the angular momenta.

In the present work, we have concentrated on collisions of DM structures with high enough relative velocities, which corresponds to the quasielastic interaction. We have also investigated the system with lower initial kinetic energy, which leads to the formation of a single localized structure after long-term evolution. The final state of the system is determined by the initial angular momenta. For example, merging vortices propagating along the vortex line with $s_1 = 1$ and $s_2 = -1$ leads to the formation of fundamental soliton $s = 0$, while in the case of $s_1 = 1$ and $s_2 = 1$ we can obtain $s = 1$ vortex structure.

In all the collisions mentioned above, especially during the merging of two fundamental solitons/vortices, we have seen complex redistribution of DM density. It is well known that such matter redistribution will generate GWs. With the fast development of GW detection techniques in recent years, such GWs, once observed, could become a new tool to investigate the properties of the relevant BEC DM. Therefore, in the next section, we investigate the GW radiation in the collision processes studied above.

V. GRAVITATIONAL WAVE RADIATION

Since the velocity of the BEC matter studied here is nonrelativistic, the energy-momentum tensor is dominated by the rest energy, i.e., the density distribution function. Consequently, we can directly use the density distribution found in Sec. IV to compute the GW luminosity. We consider quadrupole moments and related GW radiation,

and we also use the common assumption that the source-detector distance is much larger than the source size [56].

With these considerations, then the luminosity of the GW takes the standard form [57]

$$L_{\text{GW}} = C \sum_{i,j} |\ddot{I}_{ij}|^2, \quad (13)$$

where $C = \frac{G^4}{80\pi^2 c^5} \frac{m^5}{a_s^5}$ and \ddot{I}_{ij} is the third derivative of the dimensionless quadrupole moment defined in (9) with respect to the dimensionless time t .

The scaled GW luminosity L_{GW}/C for collisions studied in Sec. IV is shown in Fig. 8. It is seen that in all cases, the GW emission mainly happens when the wave functions of the colliding DM structures substantially overlap. Note that the luminosity for the considered scattering processes is suppressed when the condensate density reaches its maximum value (see Fig. 7) so that L_{GW} forms a two-peak pattern. It is remarkable that the collisions of vortices with angular momenta along z -axis produce stronger emissions of GW.

Direct detection of these gravitational waves poses significant challenges due to their extremely low frequencies. The estimate of these frequencies can be obtained by considering the collision timescale determined by R_0 (or R_1)/ v , which results in timescales of millions of years. This frequency range stands in stark contrast to the typical frequencies observed in GWs from a binary neutron star or black hole mergers, which are usually in the range of tens to a few thousand Hz [58]. Comparing these low-frequency signals to the sensitivity curves of current and near-future direct gravitational wave detectors, as shown in Ref. [59], reveals that unfortunately, such signals are beyond the lower sensitivity limit of these detectors.

However, in the case of a typical dark matter halo mass $M \sim 10^{12} M_\odot$ [57] and a boson particle mass on the order of $m \sim 10^{-22}$ [eV], the peak GW luminosity, $\max L_{\text{GW}} \approx 2.7 \times 10^{31}$ [erg/s], obtained from colliding

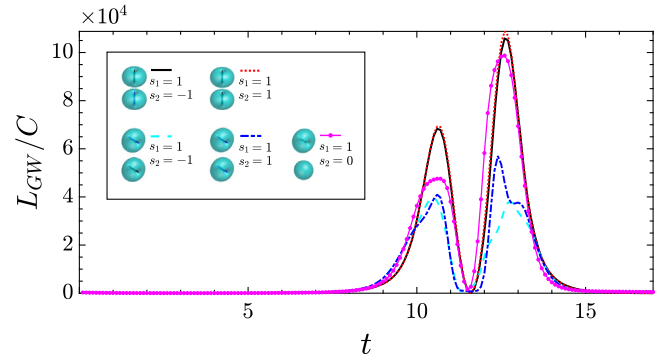


FIG. 8. The dimensionless luminosity of the gravity waves for different orientations of colliding the vortex structures shown in Figs. 4–6. Note that the luminosity of gravity waves is essentially affected by the orientation of the superflows in the DM structures.

superfluid dark matter structures aligns with the findings of Refs. [57,60]. These GWs, characterized by such luminosity and frequency, are expected to produce discernible effects on the polarization of the cosmic microwave background [57]. Consequently, future experiments hold the potential for indirectly detecting distinctive GW-induced imprints of superfluid dark matter collisions on the CMB.

VI. CONCLUSIONS

We have investigated the general properties and stability of solitonic structures of self-gravitating Bose-Einstein condensates. Previously, it was found that zero-charged and one-charged solitons are stable with respect to strong perturbations. In the present work, we reveal that these solitons survive even after head-on collision. In spite of the nonelasticity of interaction, vortex solitons demonstrate robust evolution and restore their forms after collisions. We have found that the quantum nature of the self-gravitating Bose-Einstein condensates leads to the formation of remarkable topological excitations in the form of vortex rings and Josephson vortices during the collision of the

dark matter solitonic structures. We have investigated gravitational waves radiated by interacting DM halos and demonstrated the effect of the quantum interference patterns formed by colliding BECs on GWs luminosity.

The fascinating physics of superfluid DM leads to a number of observational signatures that might help to elucidate the basic properties of dark matter particles. In particular, the existence of stable DM vortex structures can significantly affect the dynamics of luminous matter, especially near the vortex core. Detailed consideration of interactions between stable DM vortex structures and the baryonic matter may be a relevant extension of the present work.

ACKNOWLEDGMENTS

We thank Stanislav Vilchinskii and Luca Salasnich for useful discussions. Y.N. acknowledges support by the Austrian Science Fund (FWF) [Grant No. I6276]. A. Y. acknowledges support from BIRD Project ‘‘Ultracold atoms in curved geometries’’ of the University of Padova. Research of E.G., J.J., and A. Y. is supported by the China-Ukraine Project IGSCP-12.

-
- [1] M. J. Edmonds, T. Bland, R. Doran, and N. G. Parker, *New J. Phys.* **19**, 023019 (2017).
 - [2] H.-Y. Schive, T. Chiueh, and T. Broadhurst, *Nat. Phys.* **10**, 496 (2014).
 - [3] T. Matos and L. Arturo Ureña-López, *Phys. Rev. D* **63**, 063506 (2001).
 - [4] V. Sahni and L. Wang, *Phys. Rev. D* **62**, 103517 (2000).
 - [5] I. S. Goldstein, S. M. Koushiappas, and M. G. Walker, *Phys. Rev. D* **106**, 063010 (2022).
 - [6] A. Paredes, D. N. Olivieri, and H. Michinel, *Physica (Amsterdam)* **403D**, 132301 (2020).
 - [7] F. Maucher, S. Skupin, M. Shen, and W. Krolikowski, *Phys. Rev. A* **81**, 063617 (2010).
 - [8] J. Qin, G. Dong, and B. A. Malomed, *Phys. Rev. A* **94**, 053611 (2016).
 - [9] J. Qin, Z. Liang, B. A. Malomed, and G. Dong, *Phys. Rev. A* **99**, 023610 (2019).
 - [10] D. O’Dell, S. Giovanazzi, G. Kurizki, and V. M. Akulin, *Phys. Rev. Lett.* **84**, 5687 (2000).
 - [11] S. Giovanazzi, D. O’Dell, and G. Kurizki, *Phys. Rev. A* **63**, 031603 (2001).
 - [12] S. Giovanazzi, G. Kurizki, I. E. Mazets, and S. Stringari, *Europhys. Lett.* **56**, 1 (2001).
 - [13] D.-I. Choi, *Phys. Rev. A* **66**, 063609 (2002).
 - [14] C. G. Böhrer and T. Harko, *J. Cosmol. Astropart. Phys.* **06** (2007) 025.
 - [15] P.-H. Chavanis, *Eur. Phys. J. Plus* **132**, 248 (2017).
 - [16] P.-H. Chavanis and T. Harko, *Phys. Rev. D* **86**, 064011 (2012).
 - [17] L. Hui, J. P. Ostriker, S. Tremaine, and E. Witten, *Phys. Rev. D* **95**, 043541 (2017).
 - [18] P. Sikivie and Q. Yang, *Phys. Rev. Lett.* **103**, 111301 (2009).
 - [19] E. J. M. Madarassy and V. T. Toth, *Phys. Rev. D* **91**, 044041 (2015).
 - [20] N. Siemonsen and W. E. East, *Phys. Rev. D* **103**, 044022 (2021).
 - [21] A. I. Yakimenko, Y. A. Zaliznyak, and Y. Kivshar, *Phys. Rev. E* **71**, 065603 (2005).
 - [22] V. Lashkin, A. Yakimenko, and Y. A. Zaliznyak, *Phys. Scr.* **79**, 035305 (2009).
 - [23] T. Rindler-Daller and P. R. Shapiro, *Mon. Not. R. Astron. Soc.* **422**, 135 (2012).
 - [24] N. Sanchis-Gual, F. D. Giovanni, M. Zilhão, C. Herdeiro, P. Cerdá-Durán, J. Font, and E. Radu, *Phys. Rev. Lett.* **123**, 221101 (2019).
 - [25] X. Zhang, M. H. Chan, T. Harko, S.-D. Liang, and C. S. Leung, *Eur. Phys. J. C* **78**, 1 (2018).
 - [26] Y. O. Nikolaieva, A. O. Olashyn, Y. I. Kuriatnikov, S. I. Vilchinskii, and A. I. Yakimenko, *Low Temp. Phys.* **47**, 684 (2021).
 - [27] A. S. Dmitriev, D. G. Levkov, A. G. Panin, E. K. Pushnaya, and I. I. Tkachev, *Phys. Rev. D* **104**, 023504 (2021).
 - [28] E. Cotner, *Phys. Rev. D* **94**, 063503 (2016).

- [29] J. A. González and F. S. Guzmán, *Phys. Rev. D* **83**, 103513 (2011).
- [30] A. Bernal and F. S. Guzmán, *Phys. Rev. D* **74**, 103002 (2006).
- [31] D.-I. Choi, *Phys. Rev. A* **66**, 063609 (2002).
- [32] E. R. Carrasco, P. L. Gomez, T. Verdugo, H. Lee, R. Diaz, M. Bergmann, J. E. H. Turner, B. W. Miller, and M. J. West, *Astrophys. J. Lett.* **715**, L160 (2010).
- [33] D. Harvey, R. Massey, T. Kitching, A. Taylor, and E. Tittley, *Science* **347**, 1462 (2015).
- [34] A. Paredes and H. Michinel, *Phys. Dark Universe* **12**, 50 (2016).
- [35] F. S. Guzmán and A. A. Avilez, *Phys. Rev. D* **97**, 116003 (2018).
- [36] B. Schwabe, J. C. Niemeyer, and J. F. Engels, *Phys. Rev. D* **94**, 043513 (2016).
- [37] I.-K. Liu, N. P. Proukakis, G. Rigopoulos *et al.*, *Mon. Not. R. Astron. Soc.* **521**, 3625 (2023).
- [38] H.-Y. Schive, M.-H. Liao, T.-P. Woo, S.-K. Wong, T. Chiueh, T. Broadhurst, and W. Y. P. Hwang, *Phys. Rev. Lett.* **113**, 261302 (2014).
- [39] A. Maleki, S. Baghram, and S. Rahvar, *Phys. Rev. D* **101**, 023508 (2020).
- [40] R. Massey *et al.*, *Mon. Not. R. Astron. Soc.* **449**, 3393 (2015).
- [41] A. A. Avilez and F. S. Guzmán, *Phys. Rev. D* **99**, 043542 (2019).
- [42] F. S. Guzmán, J. A. González, and J. P. Cruz-Pérez, *Phys. Rev. D* **93**, 103535 (2016).
- [43] C. Palenzuela, I. Olabarrieta, L. Lehner, and S. L. Liebling, *Phys. Rev. D* **75**, 064005 (2007).
- [44] C. Palenzuela, L. Lehner, and S. L. Liebling, *Phys. Rev. D* **77**, 044036 (2008).
- [45] M. Bezares, C. Palenzuela, and C. Bona, *Phys. Rev. D* **95**, 124005 (2017).
- [46] J. Balakrishna, A numerical study of boson stars: Einstein equations with a matter source, Ph.D. thesis, Washington University in Saint Louis, Missouri, 1999.
- [47] M. W. Choptuik and F. Pretorius, *Phys. Rev. Lett.* **104**, 111101 (2010).
- [48] M. Markevitch, A. H. Gonzalez, D. Clowe, A. Vikhlinin, W. Forman, C. Jones, S. Murray, and W. Tucker, *Astrophys. J.* **606**, 819 (2004).
- [49] S. L. Liebling and C. Palenzuela, *Living Rev. Relativity* **15**, 6 (2012).
- [50] C. F. B. Macedo, P. Pani, V. Cardoso, and L. C. B. Crispino, *Phys. Rev. D* **88**, 064046 (2013).
- [51] X. Antoine, W. Bao, and C. Besse, *Comput. Phys. Commun.* **184**, 2621 (2013).
- [52] S. Costiner and S. Ta'asan, *Phys. Rev. E* **52**, 1181 (1995).
- [53] E. Munive-Villa, J. N. López-Sánchez, A. A. Avilez-López, and F. S. Guzmán, *Phys. Rev. D* **105**, 083521 (2022).
- [54] R. C. O'Reilly and J. M. Beck, *Int. J. Numer. Methods Eng.* **1** (2006).
- [55] N. Bazhan, A. Svetlichnyi, D. Pfeiffer, D. Derr, G. Birkel, and A. Yakimenko, *Phys. Rev. A* **106**, 043305 (2022).
- [56] E. Poisson and C. M. Will, *Gravity: Newtonian, Post-Newtonian, Relativistic* (Cambridge University Press, Cambridge, England, 2014).
- [57] V. Quilis, A. C. González-García, D. Sáez, and J. A. Font, *Phys. Rev. D* **75**, 104008 (2007).
- [58] B. P. Abbott *et al.* (LIGO Scientific and Virgo Collaborations), *Phys. Rev. X* **9**, 031040 (2019).
- [59] C. J. Moore, R. H. Cole, and C. P. L. Berry, *Classical Quantum Gravity* **32**, 015014 (2015).
- [60] T. Inagaki, K. Takahashi, S. Masaki, and N. Sugiyama, *Phys. Rev. D* **82**, 124007 (2010).